# THE NITROGEN ION LASER

by

C. B. COLLINS

A. J. CUNNINGHAM



Sixth

Semi - Annual Technical Report

UTDP - ML - 03

prepared for

Office of Naval Research

Department of the Navy

sponsored by

Advanced Research Projects Agency

March 1975

SECURITY CLASSIFICATION OF THIS PAGE *(When Data Entered)*

## REPORT DOCUMENTATION PAGE

READ INSTRUCTIONS BEFORE COMPLETING FORM

1. REPORT NUMBER: UTDP-ML-03
2. GOVT ACCESSION NO.
3. RECIPIENT'S CATALOG NUMBER

4. TITLE *(and Subtitle)*: THE NITROGEN ION LASER

5. TYPE OF REPORT & PERIOD COVERED: Semi-Annual Technical Rept. Period Covered 10/1/74-3/31/75

6. PERFORMING ORG. REPORT NUMBER: 1 Oct 74-31 Mar 75

7. AUTHOR(s): Carl B. Collins; Austin J. Cunningham

8. CONTRACT OR GRANT NUMBER(s): N00014-67-A-0310-0007; ARPA Order-1807

9. PERFORMING ORGANIZATION NAME AND ADDRESS
The University of Texas at Dallas
P. O. Box 688
Richardson, Texas 75080

10. PROGRAM ELEMENT, PROJECT, TASK AREA & WORK UNIT NUMBERS
NR 016-211
ARPA Order No. 1807

11. CONTROLLING OFFICE NAME AND ADDRESS
Office of Naval Research
Department of the Navy
Arlington, Virginia

12. REPORT DATE: 31 March 1975

13. NUMBER OF PAGES: 55 (12) 61 p.

14. MONITORING AGENCY NAME & ADDRESS *(if different from Controlling Office)*
Code 421

15. SECURITY CLASS. *(of this report)*: UNCLASSIFIED

15a. DECLASSIFICATION/DOWNGRADING SCHEDULE

16. DISTRIBUTION STATEMENT *(of this Report)*

Distribution of this document is unlimited

17. DISTRIBUTION STATEMENT *(of the abstract entered in Block 20, if different from Report)*

List of all receiving, per contractual requirements:
Semi Annual Technical Item No. A002

18. SUPPLEMENTARY NOTES

19. KEY WORDS *(Continue on reverse side if necessary and identify by block number)*

Nitrogen Ion Laser
Charge Transfer
Laser
$He_2^+$

391 647

20. ABSTRACT *(Continue on reverse side if necessary and identify by block number)*

The characterization of the nitrogen ion laser pumped by charge transfer from $He_2^+$ is reported in this work. Intense laser emission in the violet at 427 nm has been observed and found to have a linewidth less than 0.3 Å. The pumping ion, $He_2^+$, was produced by discharge of a fast-pulsed electron beam gun, APEX-1, into several atmospheres of a mixture of helium and nitrogen. Excitation current densities were 1.4 KA/cm$^2$ at 1 MV over a 1 x 10 cm transverse geometry. Under these conditions, the efficiency of the emission of 427 nm laser radiation was found to be proportional to the total pressure raised to the 1.2 power. (over)

DD FORM 1 JAN 73 1473 EDITION OF 1 NOV 65 IS OBSOLETE

SECURITY CLASSIFICATION OF THIS PAGE *(When Data Entered)*

Efficiencies of 1.6% relative to the energy lost by the electron beam in the radiating volume have been achieved in volumes of 16 cc. Outputs of 35 mJ have been obtained from the 16 cc working volume at 30 atm pressure.

Sixth Semi-Annual Technical Report

Item A002

Period Ending: 31 March 1975

Short Title: RECOMBINATION LASER

ARPA Order Number 1807

Program Code Number 2E90

Contract Number N00014-67-A-0310-0007

Principal Investigator: Carl B. Collins
The University of Texas at Dallas
P. O. Box 688
Richardson, Texas 75080
(214) 690-2885

Contractor: The Board of Regents of
The University of Texas System

Scientific Officer: Director
Physics Programs
Physical Sciences Division
Office of Naval Research
Department of the Navy
800 N. Quincy Street
Arlington, Virginia 22217

Effective Date of Contract: 21 March 1972

Expiration Date of Contract: 30 June 1975

| | |
|---|---|
| Amount of Contract: | $ 99,990.00 |
| Amount of Modification #1: | 91,400.00 |
| Amount of Modification #2: | 100,000.00 |
| Amount of Modification #3: | 150,000.00 |
| Total Amount: | $441,390.00 |

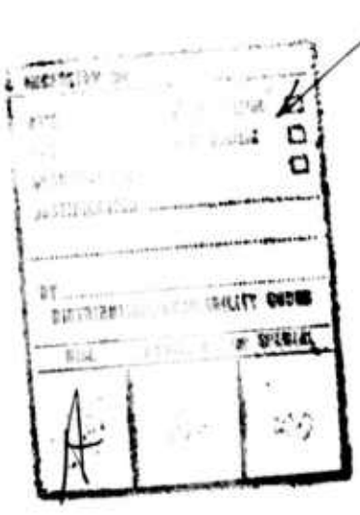

Sponsored by

Advanced Research Projects Agency

ARPA Order No. 1807

Form Approved Budget Bureau No. 22-R0293

CONTENTS

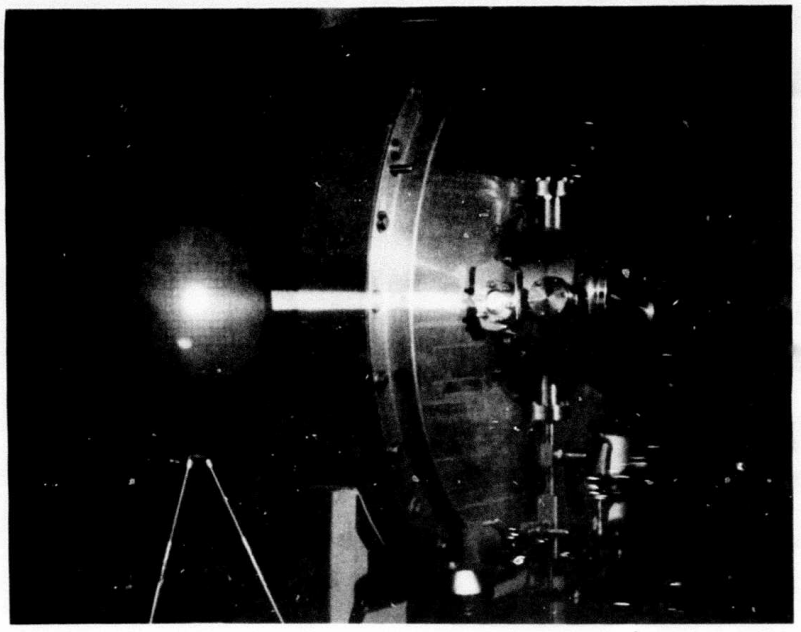

Photograph recording a single 300 KW pulse from the nitrogen-ion laser. The emission consists of a single spectral line of less than 0.3 Å linewidth at 4278 Å in the violet. The laser cavity is contained in the pressure vessel seen to the rear of the photograph. It is the most efficient visible, e-beam laser constructed to date, scaling at 1.6% of the energy deposited in the gas.

## I. TECHNICAL REPORT SUMMARY

A year ago it was proposed by Collins, et.al.[1] that resonant charge transfer reactions might provide nearly ideal pumping mechanisms for recovering one photon for each ion produced by the discharge of an intense electron beam into high pressure gases. Since the energy from an e-beam discharge can be stored at densities of the order of kilojoules per liter with efficiencies over 50%, such a pumping mechanism would clearly point toward the development of e-beam lasers operating at visible wavelengths with system efficiencies between 5 and 10%. The potential of the pumping reaction

$$He_2^+ + N_2 \rightarrow N_2^+ (B^2\Sigma_u) + 2He \qquad (1)$$

was reported in the same letter[1], together with construction of a two-pass amplifier excited by a Febetron 706 and operating at 4278, 4709 and 5228 Å. The first nitrogen ion laser pumped by charge transfer from $He_2^+$ was subsequently constructed as described in a recent letter[2]. Intense laser emission at 4278 Å was reported with an efficiency measured to be 1.8% relative to the energy lost by the electron beam in a relatively small radiating volume of 0.63 $cm^3$.

Subsequent studies of the dependence on experimental parameters of the power output have demonstrated that the nitrogen ion laser scales with pressure and volume at a rate showing a strong non-linear dependence on total gas pressure. Empirically this can be expressed as a pressure-dependent efficiency for output of the single laser line at 4278 Å measured relative to the energy lost by the electron beam in the total duration of the e-beam pulse. Data measured

over a wide range of experimental parameters was found to be closely approximated by the following expression for the efficiency, $\varepsilon$,

$$\varepsilon = 6.5\% \ (P/100)^{1.2} \quad , \qquad (2)$$

where P is the total gas pressure in atmospheres and 6.5% is the theoretical limit on efficiency. Validity of (2) was confirmed in working volumes of 10 to 20 $cm^3$ over a range of efficiencies varying from 0.3% to 1.6% as a consequence of changes in total pressure, fractional composition and mirror reflectivity. These data are summarized in Figure 1, which presents output pulse energies measured at 4278 Å as a function of input energy cost. For convenience this latter has been normalized so that energy deposition from the e-beam is numerically equal to the total gas pressure in atmospheres. On such a plot, then, lines of constant efficiency appear as diagonals and the absolute calibration is provided on each.

Both output pulse energy and efficiency increased rapidly with pressure and the dependence given by (2) can be clearly seen in the figure. The highest efficiency measured was 1.6% and was found at the highest pressure which the pressure vessel could accommodate, 28.7 atm. The corresponding energy emitted in the pulse was 36 mJ and the peak power was 2.3 megawatt.

The laser device used in these studies, ELAC-1, has been described in previous reports[3,4]. Basically it consisted of a pair of plane dielectric mirrors which were mounted to allow angular alignment, spaced with 14 cm invar rods, and contained in a stainless steel pressure vessel with quartz windows sealed across the optical axis external to the cavity. In operation the system was filled to a pressure ranging from 1 to 30 atmospheres of a mixture of helium

Figure 1

Summary plot of total laser pulse energy emitted from a 16 $cm^3$ volume as a function of relative deposition of energy from the electron beam. Units have been chosen so that the deposition is numerically equal to the total gas pressure in atmospheres. Variation of the deposition was obtained by changing the total gas pressure; hence the stopping power. The peak e-beam current was 13 KA in each case. Lines of constant efficiency appear as diagonals with corresponding values marked. Different partial pressures of $N_2$ are indicated by the shape of the data point as follows:

O - 8 Torr

X - 30 Torr

Δ - 60 Torr

□ - 120 Torr

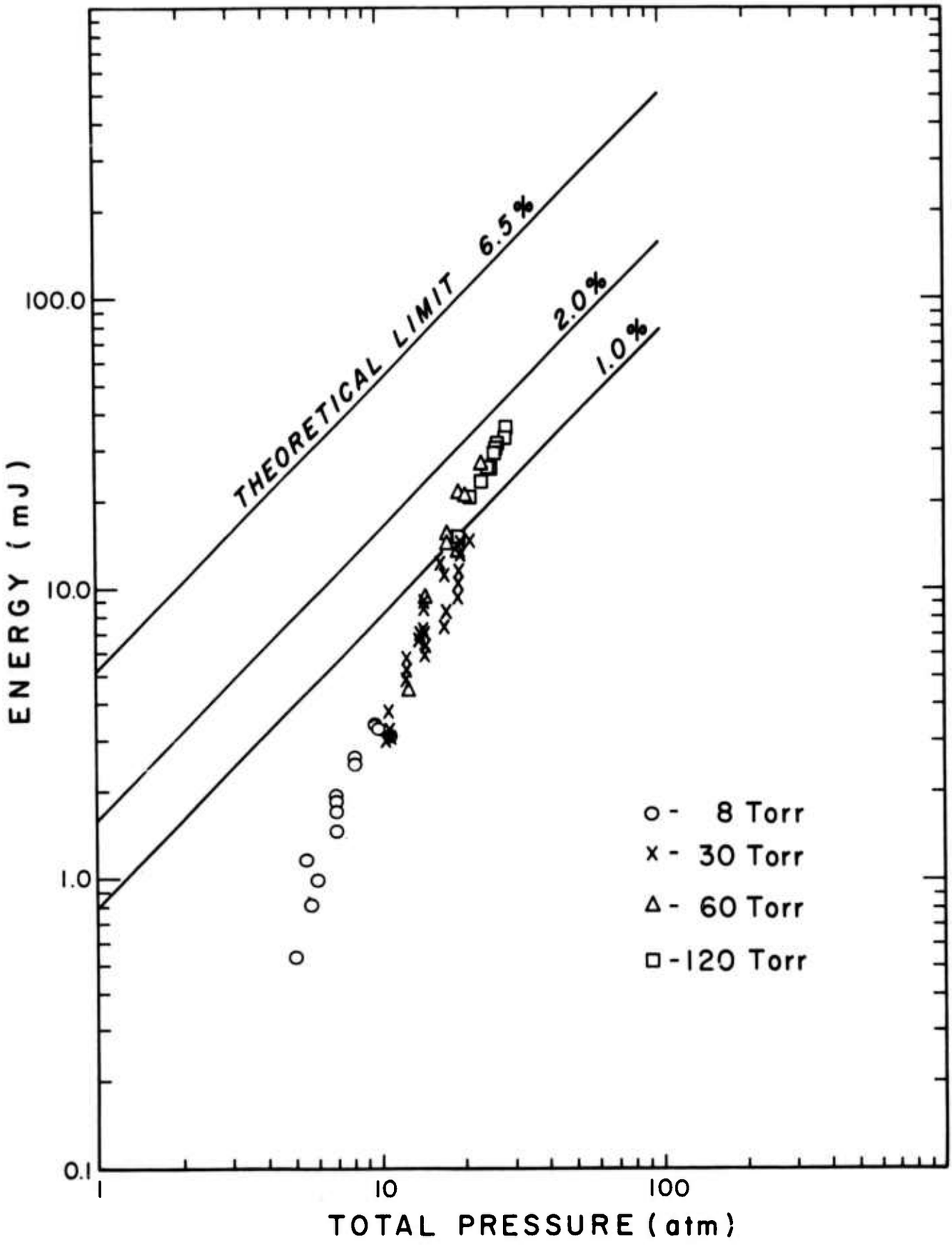
THEORETICAL LIMIT 6.5%
2.0%
1.0%
100.0
10.0
1.0
0.1
ENERGY (mJ)
1
10
100
TOTAL PRESSURE (atm)
o - 8 Torr
x - 30 Torr
Δ - 60 Torr
□ - 120 Torr

and nitrogen. Useful partial pressures of nitrogen ranged from 2 to 120 Torr. Excitation was provided by an electron beam entering through a supported, 0.002-in thick titanium foil window and propagating in a direction perpendicular to the optical axis. The cross section of the beam was 1 cm x 10 cm with the longer transverse axis coincident with the optical axis of the cavity. The electron beam was emitted by APEX-1, pulsed at 13 KA and 950 KV for a nominal duration of 20 nsec with rise and fall times of 7 nsec.

Spectra were recorded with a Spex 0.75 m spectrograph with 5μ slits. Resolution was limited in practice to about 0.3 Å by the resolution of the Polaroid film used. The time dependence and power level of the light output were measured with a calibrated ITT F-4000, S20 vacuum photodiode connected directly to a Tektronix 519 oscilloscope. Proper attenuation of the laser output was provided by calibrated neutral density filters.

In operation three laser lines have been excited in mixtures of helium and nitrogen pumped by reaction (1). Each corresponds to transitions from the same upper vibrational state, v'=0, of the $B^2\Sigma_u^+$ electronic state to different lower vibrational states of the $X^2\Sigma_g^+$ electronic state of the $N_2^+$ molecular ion. The three lines and their respective vibrational transitions are: the 3914 Å (0,0), the 4278 Å (0,1), and the 4709 Å (0,2). With the proper mirror set each has been excited individually. In principle, excitation of the (0,3) at 5228 Å is possible. The most work has been done on the (0,1) transition at 4278 Å, but since each has the same upper state, those same results should be roughly characteristic of all with the exception of the (0,0) transition which self-terminates at very early times.

Linewidths of each transition have been found to be less than 0.3 Å. The occasional excitation of interferometer modes within the output windows suggest linewidths are considerably less than the instrumental limit of 0.3 Å. With

the exception of the (0,0) transition, the output pulse durations are between 10 and 15 nanoseconds for a 20 nanosecond e-beam pulse. Laser beam divergence is around 3mR.

The most important results achieved during the current reporting are believed to be, first, that the efficiency increases, not decreases, with increasing laser power. Empirically this is summarized by equation (2). Secondly, the same high efficiencies originally found to characterize small excited volumes, 0.6 $cm^3$, adequately characterize larger volumes of 10 to 20 $cm^3$. Finally, in the case of the (0,1) and (0,2) transitions, the lower laser levels are found to be unblocked by some type of collisional process which becomes increasingly more effective at higher total gas pressures.

While it should be realized that the nitrogen ion laser is only the first example of the new class of e-beam charge-transfer lasers[1], and that other similar systems offer the possibilities of even higher efficiencies and broader selections of output wavelengths, these three results observed for the emission of 4278 Å laser radiation point to the nitrogen ion laser as a device of considerable significance and clearly confirm the importance of charge transfer reactions as laser pumping mechanisms.

## II. THEORY

The development of intense pulsed electron beam sources in the 1 to 100 Gigawatt class have made feasible the deposition of energy in the form of ionization into large volumes of plasma with system efficiencies around 50%. Given an elementary mechanism utilizing this ionization and leading to the inversion of population at quantum efficiencies which are typically 10 to 20%, overall radiative efficiencies of the order of 5 to 10% can be realistically projected, provided the plasma constituents are arranged to allow for the domination of the desired reaction channel. The xenon excimer laser[3,4] is the best example of such a system in which the primary mechanism is the dissociative recombination of the $Xe_2^+$ ion. Though superficially similar, the electron beam excited pure $N_2$[7] and $H_2$[8] lasers do not actually utilize the primary ionization of the plasma; consequently, system efficiencies are reduced by orders of magnitude.

Evidently, charge transfer between the population of primary ions and a minority constituent of lower ionization potential offers a nearly ideal mechanism[1] for ultimately obtaining one photon per primary ion. If the minority constituent is selected to have the energy of an excited state of its ion approximately equal to that of the primary ion, in principle, one photon per ion can be realized with a quantum efficiency, E, equal to

$$E = \frac{IP(1)-IP(2)}{IP(1)} \qquad (2)$$

where IP(1) and IP(2) are the ionization potentials of the primary and secondary constituent, respectively. Table 1 summarizes examples of possible system efficiencies characteristic of various permanent gases diluted in helium.

TABLE I

Projected system efficiencies for the emission of radiation following charge transfer excitation from the helium molecular ion, assuming a 50% efficiency for the production of ionization by electron beam impact.

| Minor Constituent | Overall Efficiency |
|---|---|
| $N_2$ | 11.0% |
| $O_2$ | 12.5% * |
| CO | 14.5% |

*The resonant transition does not terminate on the ground state of the molecular ion.

Similar possibilities occur with other primary species, but at efficiencies reduced by the lower ionization potential of those species.

Both the available output energy and pulse duration depend strongly on partial pressures, and the high values of charge density which become feasible with e-beam excitation are needed. The deposition of energy into a high pressure gas by an electron beam is a very complex problem, and most characterizations of the process have been made for the excitation of dense inert gases. In such systems as xenon, beam-plasma effects rapidly dominate with the return currents[9,10] playing a large role.

However, an essential factor in understanding of the energy deposition from the beam lies in the fact that scattering and stopping power do not have the same dependence on atomic number, $Z$[11]. As a consequence, it is possible to have a situation in which a considerable fraction of beam energy is stopped without appreciable scattering or conversely that the scattering is so great that the simple approximation of the product of the stopping power and penetration depth seriously underestimates energy deposition, even for small fractional losses of beam energy.

The almost singular case of the light inert gases excited at beam currents below 20KA falls into the first category, and simplifying assumptions exist which render the problem tractable. Subject to limitations on the product of gas density and beam penetration depth, discussed in previous work,[3,4] the problem can be resolved into that of the differential energy loss in the gas of β-particles in a beam, the morphology of which is completely determined by the foil window through which the beam has entered. For a titanium foil, .002" thick, the following bounds on the domain of gas transparency are obtained,

$$PX\ (\text{Helium}) \leq 273\ \text{atm. cm} \qquad (4a)$$

$$PX\ (\text{Argon}) \leq 4.3\ \text{atm. cm}\ , \qquad (4b)$$

where P is the gas pressure in atmospheres and X is the penetration depth of the beam into the gas.

It can be seen from these results that, whereas the simplifying assumptions break down for argon (Z=18) at an inch of penetration at two atmospheres, they remain valid in helium (Z=2) over the entire span of parameters required for practical operation of a small test laser device. For example, at 30 atmospheres pressure, the simplified model is valid to at least 9.1 cm depth of penetration which is sufficient to describe about a half liter volume excited by a 1 x 10 cm electron beam of divergence characteristic of transmission through a .002" titanium foil window at 1 MeV for currents less than 20 KA. At higher currents, the "drag e.m.f."[10] resulting from the return currents should be considered.

Subject to the following restrictions,

$$E \leq 1 \text{ MeV} \tag{5a}$$

$$I_o \leq 20 \text{ KA} \tag{5b}$$

$$PX \leq 280 \text{ atm. cm} \quad , \tag{5c}$$

the energy deposition in helium has been calculated[3,4] to be

$$d\varepsilon\ (X,E_o) = \frac{I_o\ (t)\ [1\text{-Att}\ (E_o)]}{10 + [11 \tan \bar{\psi}\ (E_o) + 4/3 \tan^2 \bar{\psi}\ (E_o)]X}$$

$$\left\{ - \frac{dE}{dx}\ (E_o)\ (\cos\bar{\psi}(E_o))^{-1} \right\} dt \quad , \tag{6}$$

where $d\varepsilon(X,E_o)$ is the energy deposition per unit volume in the gas, $I_o$ and $E_o$ are the e-beam current and energy incident upon the foil window, dE/dx is the differential stopping power[11], Att $(E_o)$ is the attenuation coefficient of the foil at the beam energy, $E_o$, and $\bar{\psi}(E_o)$ is angle of the mean electron path deflection caused by the foil window at the same beam energy. Though seemingly complex, equation (6) can be integrated over the time-dependent beam energy and expressed in a convenient form by additionally assuming that the beam current and energy are related through an effective system impedence, $\Omega$,

$$I_o(t) = \frac{1}{\Omega} E_o(t) \tag{7}$$

Then for a linearized dependence of $E_o$ on time given by

$$E_o(t) = \begin{cases} t/\tau_r & \text{MeV} \quad \text{for } t < \tau_r \\ 1 & \text{MeV} \quad \text{for } \tau_r < t < T \\ (1-((t-T)/\tau_f)) & \text{MeV} \quad \text{for } T < t < T + \tau_f \end{cases} \quad , \qquad (8)$$

the total energy per unit volume deposited by the beam can be expressed[4] as

$$\varepsilon = 8.65\tau_r/\Omega + 18.05\ (T-\tau_r)/\Omega + 8.65\ \tau_f/\Omega \ \text{(Joules/liter/atm)} \quad . \qquad (9)$$

For example, computing for the nominal APEX-1 output used in these experiments $\tau_r = \tau_f = 6.6$ nsec., $T = 20$ nsec, $E_o = 1$MeV and

$$\Omega^{-1}/I_{max} = 10^{-3}\ (KA)^{-1} \quad . \qquad (10)$$

Then

$$\varepsilon = 0.356 \text{ Joules/liter/atm/KA} \quad . \qquad (11)$$

This value is presented for illustrative purposes only, and actual values used in calibrating the efficiency data were obtained from Faraday cup data as discussed in the next section. The values of deposition obtained can be related to the ionization produced by recognizing that the energy

cost per ion in helium[12] is 42.3 eV and that 1 Joule/ℓ will produce 1.478 x $10^{14}$ ions/$cm^3$. The energy stored as ionization is 24.5 eV per ion so that the efficiency of energy storage is

$$\text{Eff} = 57.9\% \tag{12}$$

Table 2 summarizes the energy storage which can be achieved in helium excited by APEX-1, nominally a 100 KA, 1MeV, e-beam device pulsed typically for 20 nsec FWHM with 6.6 nanosecond rise and fall times.

TABLE 2

Summary of the energy density stored as ionization in high pressure helium following discharge of APEX-1. The efficiency of the storage relative to the total energy deposited by the beam is 57.9%.

| | Energy Density (Joules/Liter) | |
|---|---|---|
| Beam Current | 20 KA | 100 KA |
| Pressure | | |
| 3 atm | 12.4 | 62 |
| 30 atm | 124 | 620 |

The ionization produced can be obtained from Table 2 by noting that 1 Joule/ℓ stored as $He^+$ represents 2.55 x $10^{14}$ ions/$cm^{-3}$. According to (12) an elementary mechanism utilizing this ionization and leading to the inversion of population would make possible overall radiative efficiencies about half of the absolute quantum efficiency of the transition. In the visible wavelength region, this would mean efficiencies between 5 and 10%, provided

the plasma constituents could be arranged to allow for the domination of the desired reaction channel.

Evidently, a resonant charge transfer reaction between the population of primary ions in the plasma and a minority constituent of lower ionization potential offers a nearly ideal mechanism for ultimately obtaining one photon per primary ion. Figure 2 presents the energy level diagrams of the ions of helium and nitrogen. Studies[13] on low pressure charge transfer mixtures have shown the strong development of spectra from molecular ion levels in near resonance with the primary helium ions. One such selectively excited transition is indicated by the arrow in Figure 2. Particular charge transfer reactions are of the form

$$He^+ + XY \rightarrow (XY^+)^* + He \qquad (13a)$$

$$\rightarrow X^+ + Y + He \qquad (13b)$$

and

$$He_2^+ + XY \rightarrow (XY^+)^* + 2He \qquad (14)$$

where the asterisk indicates additional electronic excitation. Although quantum efficiencies are more favorable for reactions excited by $He^+$, in practice the importance of channel (13b) in the case of $N_2$ minimizes the importance of the $He^+$ ion.

At sufficiently high pressure, the $He^+$ is rapidly converted to $He_2^+$ by the termolecular reaction

$$He^+ + 2He \rightarrow He_2^+ + He \qquad (15)$$

with a characteristic lifetime of

Figure 2

Energy level diagrams for the ionic states of helium and molecular nitrogen.

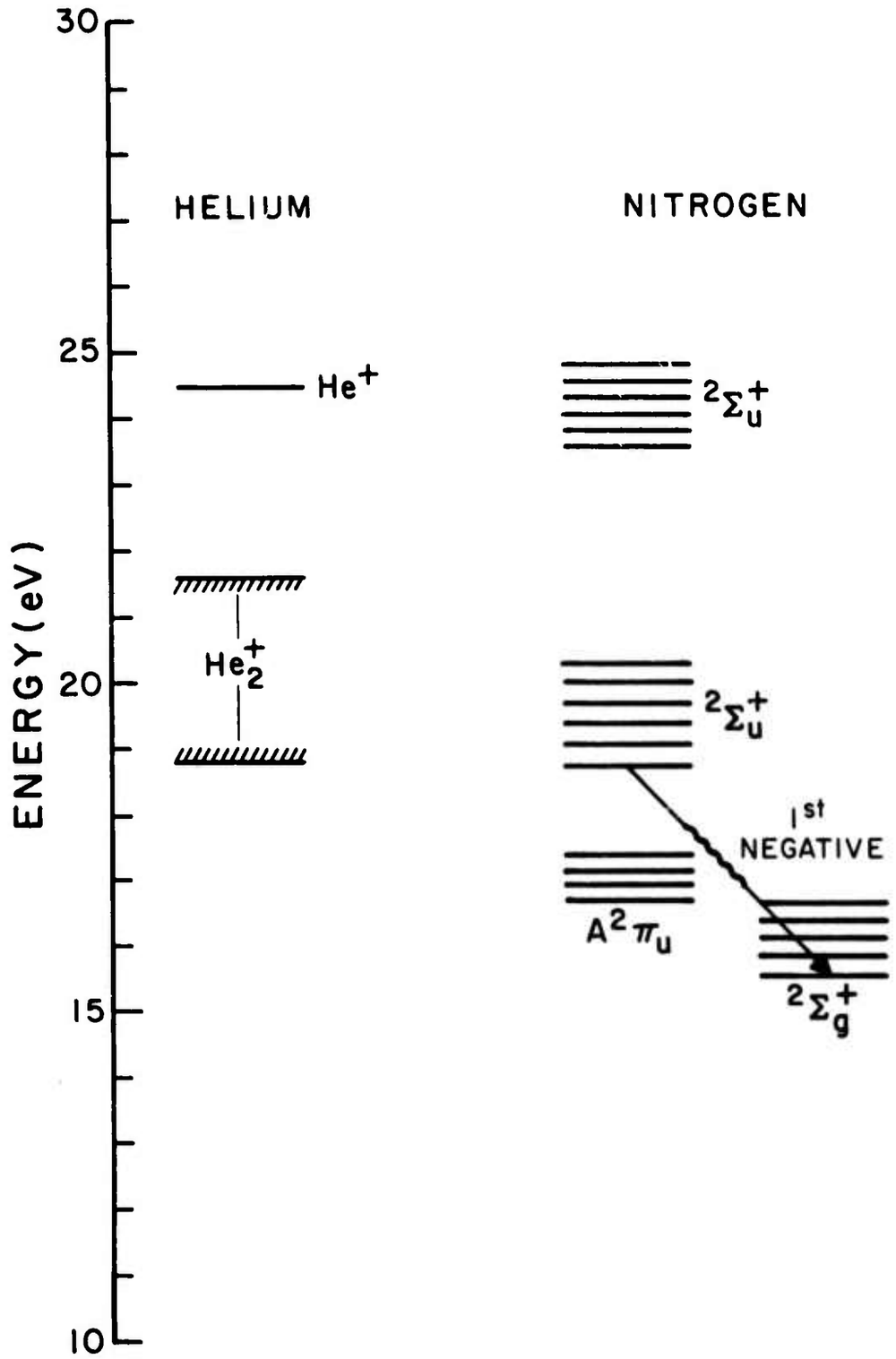
30
25
20
15
10
ENERGY (eV)
HELIUM
NITROGEN
He+
He2+
2Σu+
2Σu+
1st
NEGATIVE
A2πu
2Σg+

$$\tau = \frac{27}{p^2} \text{ nsec} \quad [14] \tag{16}$$

where p is in atmospheres. Provided the partial pressure of minority constituent is not too great for reaction (15) to go to completion, the ionization will convert from $He^+$ to $He_2^+$, thus making available the charge transfer reaction

$$He_2^+ + N_2 \rightarrow (N_2^+)^* + 2He \quad . \tag{17}$$

This reaction[15] has a rate coefficient of about $10^{-9}$ $cm^3$ $sec^{-1}$ as does the analogous reaction[16] with $He^+$.

Requiring, then, a low enough partial pressure of minority gas so that reaction (15) can reach an $(1-e^{-1})$ end-point yield in competition with the competing channel for the loss of $He^+$ through unwanted charge transfer sets the upper limits on the partial pressures shown in Table 3.

TABLE 3

Partial pressures of He and diatomic admixtures to allow for a conversion of a fraction of $(1-e^{-1})$ of $He^+$ to $He_2^+$ in competition with charge transfer of $He^+$ and the resulting charge transfer lifetimes.

| He | Max Admixture | Charge Transfer Lifetimes |
|---|---|---|
| 3 atm | 5.9 Torr | 5.3 nsec |
| 30 atm | 590 Torr | 0.05 nsec |

Assuming that the lifetime of the source term for the minority excited states limits the rate at which energy can be extracted from the plasma through a stimulated transition, the minimum pulse widths can be computed from the partial pressures and these are shown in Table 3 above.

Referring back to Fig. 2, the probable wavelength and, hence, overall efficiency can be estimated. Both from a resonance argument and from prior observations[13] on lower pressure mixtures, the probable reaction products from (17) can be identified as $N_2^+(B^2\Sigma_u^+)$. The most probable transition is the (0,1) vibrational component of the $B \rightarrow X$ transition at 4278 Å. This corresponds to a 2.90 eV photon or an equivalent absolute quantum efficiency relative to the $He^+$ ion at 24.5 eV of 11.8%. This value together with expression (12) for the efficiency for the production of $He^+$ gives an overall efficiency Eff($\lambda$) of

$$\text{Eff. } (4278\ \text{Å}) = 6.8\% \quad , \tag{18}$$

assuming reaction (15) goes to completion so that one photon per ion is realized.

From the above considerations, it appears peak power densities of the order of a Gigawatt per liter should be available to potential laser transitions for reasonable values of experimental parameters, provided the requisite population inversions occur. Considering only the better known $N_2^+$ system, the Einstein B-coefficient for absorption and stimulated emission can be written[17] as

$$B = \frac{1}{8\pi hc\nu^3} \quad \frac{g_n}{g_m} \quad \frac{1}{\tau} \tag{19}$$

where it is assumed the upper state is n and the lower, m; $\nu$ is in $cm^{-1}$ and the g's are degeneracies, and for the $N_2^+(^2\Sigma_u^+ \rightarrow {}^2\Sigma_g^+)$ the lifetime for spontaneous emission, is[18]

$$\tau = 66 \text{ nsec} \quad . \tag{20}$$

The expression for the amplification or absorption of radiation for an optical path length $\Delta x$ in these units is[17]

$$\Delta I = I_o \cdot \Delta x \frac{Bh\nu}{\Delta\nu} \quad \frac{g_m}{g_n} \quad N_n \left(1 - \frac{g_n}{g_m} \frac{N_m}{N_n}\right) \quad , \tag{21}$$

and leads finally[4] to

$$\kappa_o = \frac{\lambda^2}{8\pi c \Delta\nu_o} \frac{1}{\tau} \; N_n \; (1 - \frac{g_n}{g_m} \; \frac{N_m}{N_n}) \qquad . \qquad (22)$$

This expression must be corrected to reflect the molecular structure of the transition by replacing $\tau$ with the inverse of the A-coefficient times the Franck - Condon factor, $f^+ \; (\nu', \nu'')$ and by replacing the population of the upper state with the fraction of population in the most populated rotational component

$$N_n(Jmax) = \frac{2J_m+1}{Z_r} \; N_n \qquad , \qquad (23)$$

where $Z_r$ is the rotational partition function[19]

$$Z_r = \frac{\kappa T}{hcB_\nu} \qquad , \qquad (24)$$

$\kappa T$ is the average rotational energy and $B_\nu$ is the spacing parameter for rotational levels. For the B-X band $J_m \sim 8$ and from tabulated[20,21] spectroscopic constants $(2J_m+1)/Z_r = .134$, and $f^+ \; (0,0)A = 1.24 \times 10^7$, $f^+(0,1)A = 2.20 \times 10^6$, $f^+ \; (0,2)A = 5.01 \times 10^5$, and $f^+(0,3)A = 1.05 \times 10^5 \; sec^{-1}$.

To evaluate expression (22) for the various experimental conditions requires an assumption about the branching ratio for the yield of reaction (17). A lower limit can be obtained for the gain by ignoring the resonant nature of the excitation which favors the upper $B^2\Sigma_u^+$ state and assuming equal partition into the upper B and lower $X^2\Sigma_g^+$ states with the distribution among vibrational levels proportional to the Franck-Condon factors from the ground

state of $N_2$ to the B and X states of the ion.

Collecting terms (22) becomes

$$\kappa_o \text{ max } (\nu', \nu'') = \frac{\lambda^2}{8\pi c \Delta\nu_o} \text{ Af}^+ (\nu',\nu'') \quad (1-e^{-1}) \text{ X}$$

$$\frac{1}{2} \frac{(2J_m+1)}{Z_r} N_e f^B (\nu',0) \left(1 - \frac{g_n}{g_m} \frac{f^X(\nu'',0)}{f^B(\nu',0)}\right) \qquad (25)$$

where $N_e$ is the initial charge density. Values for $f^B$ and $f^X$ are given by Nicholls.[21]

Then, provided the lifetime for charge transfer into the states as shown in Table 3 is significantly less than the natural radiative lifetime of 66 nsec., the information from Table 2 can be used with expression (25) to give the expected small signal gain per cm. In this evaluation, the linewidth $(\Delta\lambda o)^{-1}$ has been set to 1 $cm^{-1}$ to facilitate scaling by the unknown pressure-broadened linewidth, and resulting entries in Table 4 should be reduced by the actual linewidth in $cm^{-1}$. Values resulting from (25) have been halved to account for the nearly equal division of line strength between P and R branches of the spectrum.

TABLE 4

Expected gain coefficients for the $He:N_2$ plasmas parameterized in Table 2 for 20 KA excitation. Gains should be scaled by the inverse pressure--broadened linewidth $(\Delta\lambda o)^{-1}$ in $cm^{-1}$.

| Wavelength | 3914 Å | 4278 Å | 4709 Å | 5228 Å |
|---|---|---|---|---|
| $(\nu',\nu'')$ | (0,0) | (0,1) | (0,2) | (0,3) |
| Helium Pressure (Atm) | | | | |
| 3 | -.0038 | .057 | .018 | .0045 |
| 30 | -.038 | .57 | .18 | .045 |

Even in the low pressure case, the gains are high enough after the reduction in the tabulated values because of the pressure broadening to permit the extraction of stimulated emission from the plasma. Thus, the elements of the theory are sufficient to show that charge transfer reactions should provide useful laser pumping mechanisms.

Evidently this model is overly conservative in its estimate of equal branching between the upper and lower electronic states. Recent experiments, to be discussed in the next section, have shown strong laser emission from the (0,0) transition in disagreement with the above model. This implies that the resonant behavior of reaction (17) is a dominant factor and equation (25) needs to be adjusted upward.

Nevertheless, the results of Table 4 indicate that, at some time after the onset of the growth of ionization in the electron beam produced plasma, the threshold for lasing can be satisfied for a cavity of practical characteristics. At that point, it can be expected the cavity will oscillate, and the resulting stimulated emission will dump as laser radiation the stored energy corresponding to the fraction of $He^+$ converted to $N_2^+$ B state molecules by that time. From Table 2 it can be seen that this output energy could be as large as 73 Joules/liter at 100 KA and 30 atm and could represent 6.8% of the energy lost by the beam in the radiating volume. However, this assumes the gas mixture can be perfectly optimized. In practice, the filling of the lower $X^2\Sigma_g^+$ states by spontaneous emission, unfavorable branching and chemical and electrical quenching of the B state will determine a maximum effective time, $\tau_M$ over which the charging function can be integrated to yield stored energy that can be recovered with the modelled efficiency. Because of the importance attached to describing these limiting effects, further refinement of the model to derive $\tau_M$ is being undertaken at this time.

However, it is important to recognize that the potentially limiting mechanisms are minimized in the charge transfer scheme described here. In this fact lies the primary advantage in this mechanism. It results largely from the large cross sections[16], $10^{-14}$ $cm^2$, characteristic of such processes. This is to be compared with the value of $0.05 \times 10^{-14}$ $cm^2$ characteristic of the argon-nitrogen reaction recently reported[22] to lead to laser emission in argon-nitrogen mixtures. These values for the charge transfer process are at least an order of magnitude larger than those characteristic of most excitation transfer reactions involving neutral atomic and molecular species. This means much smaller concentrations of the gas to be excited can be used which, in turn, means that chemical quenching of the final excited state population should be virtually negligible, as seems to be the case in the nitrogen ion laser finally realized.

## III. THE NITROGEN ION LASER, PHENOMENOLOGY

As mentioned in the introductory section, it was first demonstrated about a year ago[1] that resonant charge transfer held considerable promise as a potential laser pumping mechanism. Direct measurements of gain obtained with a tunable dye laser were reported at that time. Lasing was reported a few months later.[2,3] Outputs were small, 9 KW, but efficiencies were around 1.8%. However, excited volumes were quite small, 0.63 $cm^3$, and the first concern upon receipt of the electron beam source at our facility was to determine the scalability of this result to larger volumes more nearly corresponding to the use of the entire e-beam cross section.

The subsequent series of experiments reported in the previous report[4] served to raise outputs to 325 KW and lower efficiencies. Complicated effects resulting from the non-linearity of the reaction sequence tended to confuse the early phenomenology.

This report concerns the resolution of many of these effects. As will be discussed, output variation with mirror reflectivity, gas composition, and problems of energy deposition from the beam will be considered. As will be shown, the resolution of these effects allows all data acquired to date to be reconciled with the pressure-dependent efficiency modeled empirically by expression (2).

A. Energy Deposition - Excitation of the charge transfer plasmas used throughout this phase of the research was produced by the APEX-1 electron beam device acquired under this contract.

The APEX-1, electron beam gun was constructed by Systems, Science and Software of Hayward, California. It is a fast pulse, sheet beam gun emitting

100 KA pulses of 1 MeV with a 1 x 10 cm transverse cross section. Pulse durations are typically 20 nanosecond FWHM with a 6.6 nanosecond rise time and a fall time controlled by a shorting electrode. By proper adjustment, the fall time can be reduced to less than 7 nsec. During the experimental series reported here, the anode-cathode spacing in the output diode was increased to give a larger diode impedance and consequent peak current around 13 KA. Larger currents were not attempted as the operation under those conditions is rendered difficult by problems of foil survivability.

The afterglow chamber used in these experiments was the ELAC-1 device described previously[4]. It consisted of a laser cavity mounted to a foil support assembly and contained in a cylindrical high pressure vessel with axis of symmetry along the axis of beam propagation as shown in Figure 3. The assembly was constructed of UHV-grade stainless steel with windows and gas handling connections made with Varian-type copper shear seals. The laser cavity consisted of a pair of dielectric mirrors which were mounted to allow angular alignment, spaced with 14 cm invar rods, and contained in the pressure vessel with sapphire or quartz windows sealed across the optical axis external to the cavity as shown in Figure 3.

In operation the system was pressurized with 1 to 30 atmospheres of a mixture of helium and nitrogen. Useful partial pressures of nitrogen ranged from 2 to 120 Torr. Excitation was provided by the electron beam from APEX entering through a supported, 0.002-in thick titanium foil window and propagating in a direction perpendicular to the optical axis.

Current density in the electron beam was measured with a calibrated Faraday cup replacing the pressure vessel and laser cavity. Particular attention was paid to relative timing and cable lengths so that the temporal relation between

Figure 3

Exploded view of the e-beam laser afterglow chamber (ELAC-1) supporting the nitrogen ion laser work described here.

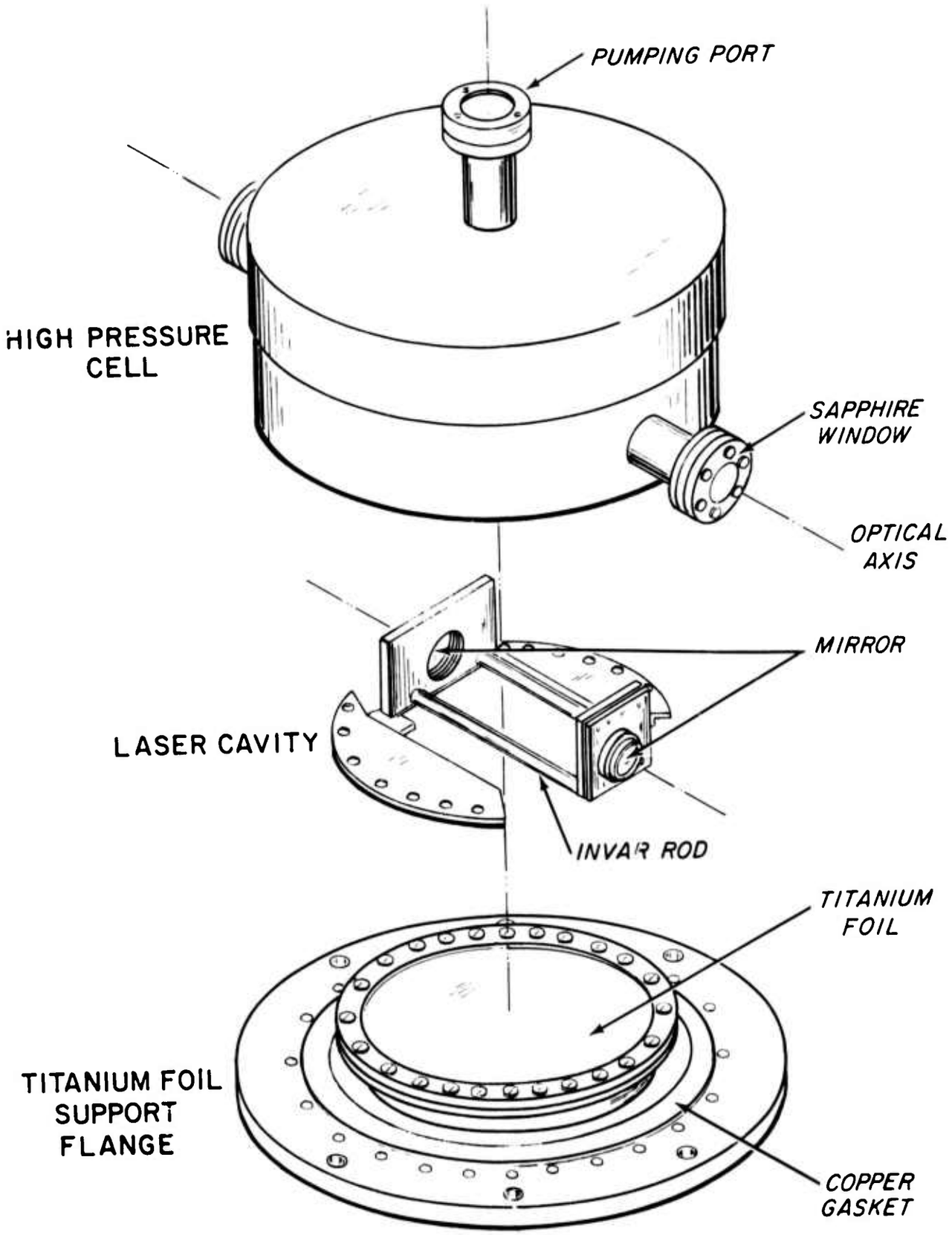
PUMPING PORT
HIGH PRESSURE CELL
SAPPHIRE WINDOW
OPTICAL AXIS
MIRROR
LASER CAVITY
INVAR ROD
TITANIUM FOIL
TITANIUM FOIL SUPPORT FLANGE
COPPER GASKET

beam current and laser output could be determined subsequently. Output from the Faraday cup was directly recorded with the 519 oscilloscope. Figure 4 shows a record of the "standard" e-beam pulse used during the parameterizations of the laser output. Reproduceability was good and Figure 4 shows three possible linear "fits" to the same trace which facilitate the use of equation (9) for the calculation of energy deposition. Each possible fit yields a different set of $\Omega$ and $\tau$ parameters. However, the resulting deposition values, shown to the right of each trace, yield only small dependence of deposition on the particular fit. The value of 4.8 J/liter/atm was accepted for the subsequent calibrations of output efficiency. During these measurements the outputs were not artificially shortened through the use of the clipping option available on APEX-1.

B. Effects of Mirror Geometry - Initial examination of the raw data relating laser pulse energy to e-beam deposition does not reveal a trend suggesting the nature of the dependence of output on the various diverse experimental parameters. Figure 5 illustrates this point, presenting results obtained with a variety of gas compositions and mirror reflectivities. Each datum has three common features, a standard excitation pulse, a plane-parallel optical cavity, and the emission of the single laser line at 4278 Å.

Although the plane-parallel optical cavity appears, a priori, the most attractive in terms of analysis, in fact this is only the case for CW oscillation after stable cavity modes have developed. The transient response of such cavities to self-excitation is complex. Consider, for example, that the cavity is initially excited by spontaneous emission at a point on the axis near one of the mirrors. Then, after three transits of the cavity, for example, the situation is represented schematically in Figure 6.

Figure 4

Recording from a 519 oscilloscope of the time-dependence of the electron beam current for the "standard pulse" used in the efficiency measurements. Also shown are three possible linear approximations to the same data, normalized in area. To the right of each trace is given the resulting energy deposition together with the value appropriate for the 16.2 $cm^3$ "standard volume." Zero time for this illustration is arbitrary.

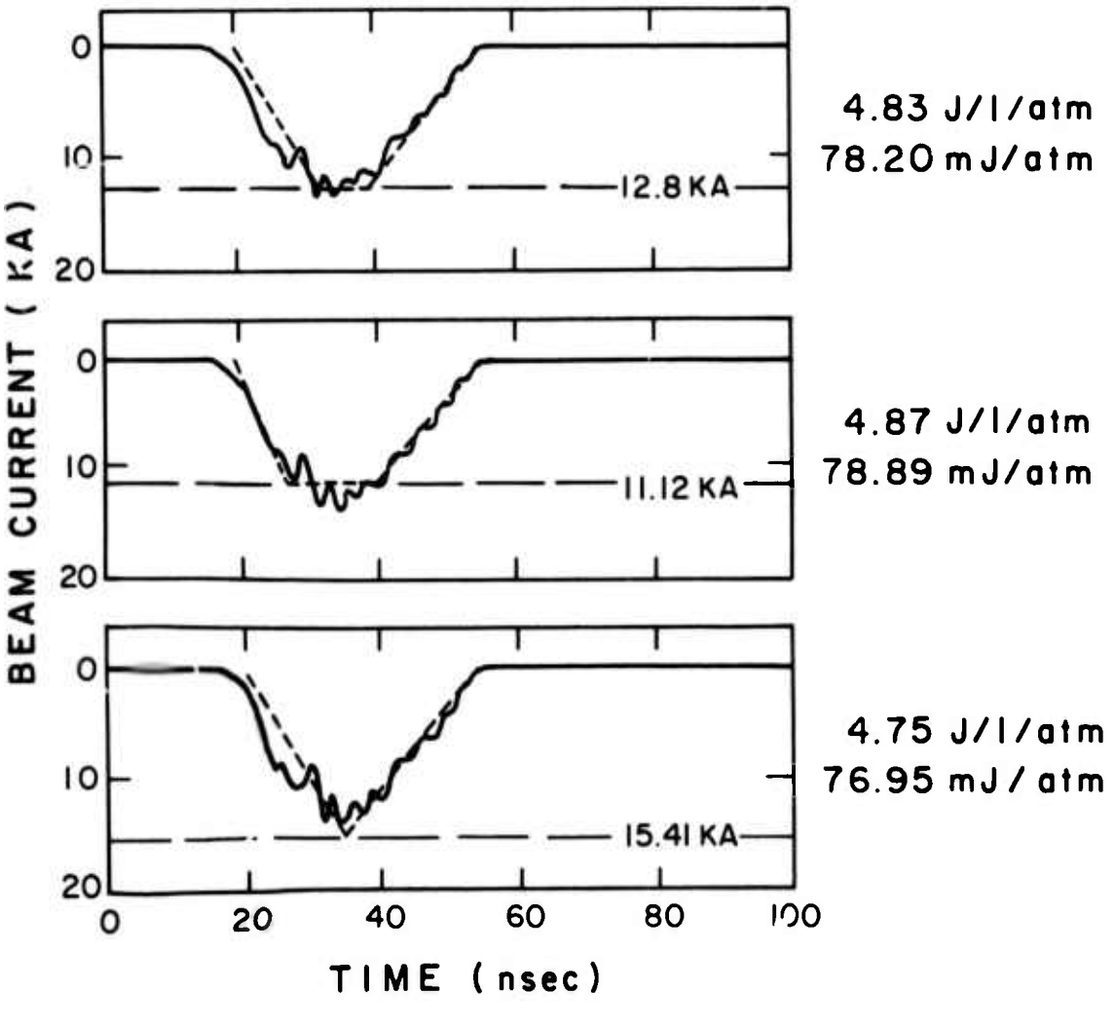
BEAM CURRENT ( KA )
0
10
20
12.8 KA
11.12 KA
15.41 KA
0
20
40
60
80
100
TIME ( nsec )
4.83 J/l/atm
78.20 mJ/atm
4.87 J/l/atm
78.89 mJ/atm
4.75 J/l/atm
76.95 mJ/atm

Figure 5

Summary plot of total pulse energy emitted from a 16 $cm^3$ volume as a function of relative deposition of energy from the electron beam. Variation of the deposition is obtained by changing the total gas pressure; hence the stopping power. The peak e-beam current is 13KA in each case. Lines of constant efficiency appear as diagonals. The partial pressure of nitrogen in Torr used in each series is shown and the difference between open and filled symbols is made by a difference in mirror characteristics.

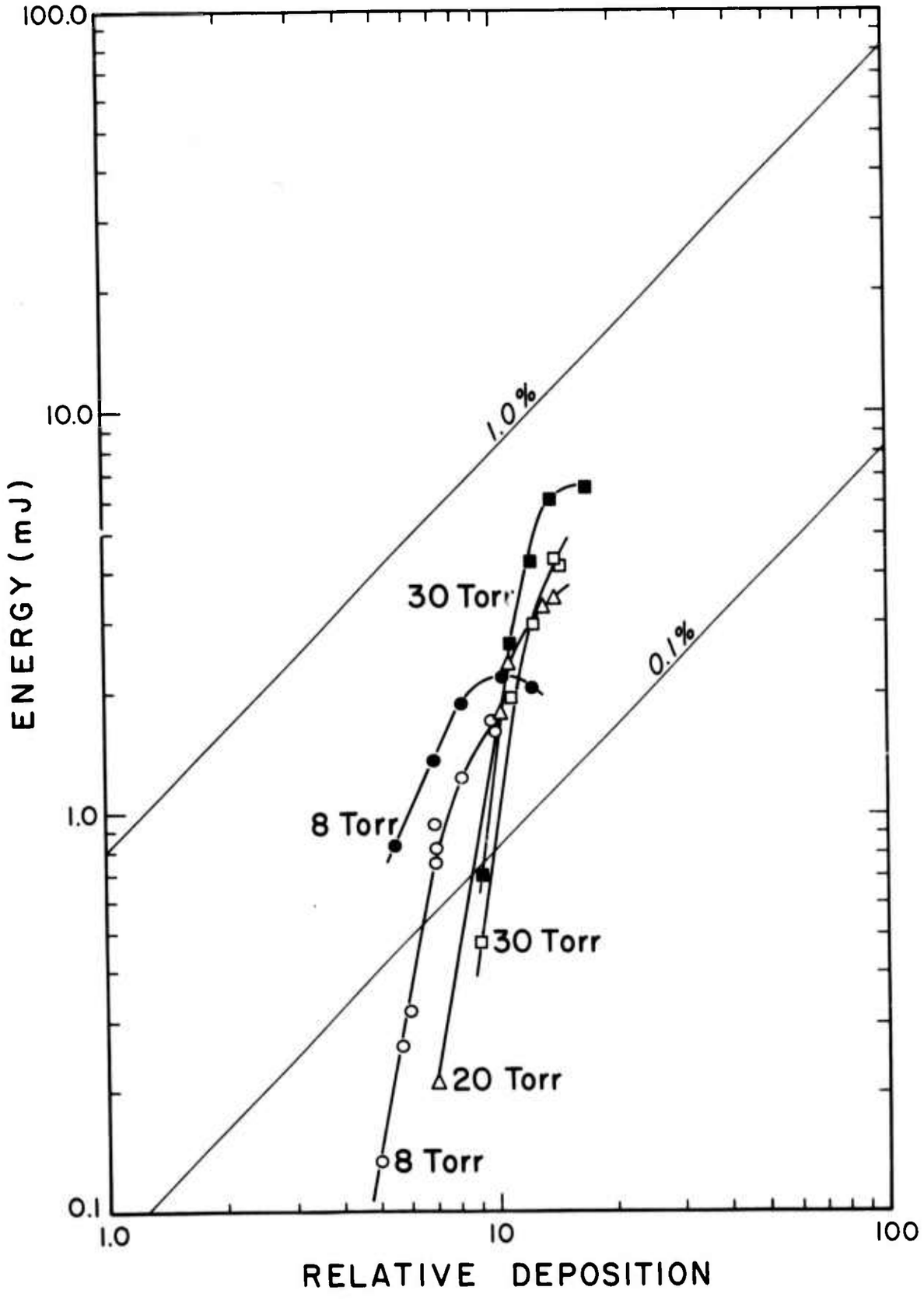
100.0
10.0
1.0
0.1
ENERGY (mJ)
1.0
10
100
RELATIVE DEPOSITION
1.0%
0.1%
30 Torr
8 Torr
30 Torr
20 Torr
8 Torr

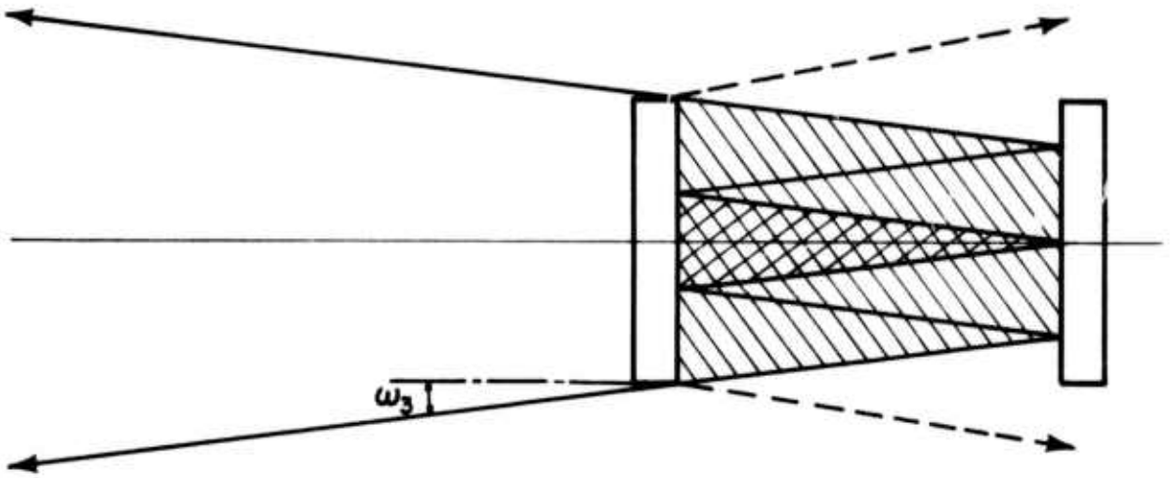


Figure 6

Sketch of the geometry of a plane-parallel , self-excited laser cavity showing the growth of modes.

Several points are to be observed. First, of the energy, $E_3$, circulating within the cavity at the end of the third pass, a fraction T x $E_3$ will be emitted into the output beam with divergence $\omega_3$, and the remainder (1-T) x $E_3$ will be reflected to begin a fourth pass. Of that part reflected, a fraction, $W_3$, will miss the opposite mirror and contribute to the walk-off loss. To the remainder, $(1-W_3)$ x (1-T) x $E_3$, which will successfully complete a fourth pass, an increment, $\Delta E_3$ will be added by stimulated emission, provided the population inversion exists at that time.

Working backward, then, the energy, $E_3$, circulating at the end of the third pass and leading to the energy detected in the beam at that time is the sum of three increments, $\Delta E_i$, extracted from various volumes of the plasma and surviving losses (i.e. neither walking-off nor being emitted) incurred during the previous two passes. For example, whatever part of $\Delta E_1$ which survived three passes must have been extracted from the cross-hatched volume shown in Figure 6. That volume might be reasonably denoted $V_{Nn}$, the volume from which the $n^{th}$ increment surviving walk-off to circulate on the $N^{th}$ pass was extracted. The corresponding energy increments, $\Delta E_{Nn}$, then represent that part of the $n^{th}$ increment surviving to contribute to the total, $E_N$, circulating at the end of the $N^{th}$ pass. Since the energy increments, $\Delta E_{Nn}$, represent directly the useful laser energy extracted from the plasma, a reasonable expression for the average volume from which the energy emitted into the beam on the $N^{th}$ pass was extracted is

$$\bar{V}_N = \sum_1^N V_{Nn} \Delta E_{Nn} / \sum_1^N \Delta E_{Nn} \quad . \qquad (26)$$

Notice that for the special case of a constant rate of energy extraction $\bar{V}_N$ becomes equal to the volume of plasma lying within a cone having one mirror

for a base and its apex touching the surface of the other mirror. For the 1 inch optics used in these experiments this would correspond to a 16.9 $cm^3$ average volume, if the mirrors were placed precisely at the edges of the 10 cm width of the e-beam. The fact that the mirrors are mounted 2 cm back from the edges of the path of the e-beam tends to reduce this number somewhat.

The converse case of CW operation is a special case which deserves mention in passing. As N increases, $\omega_N$ decreases until it approaches $\omega_o$, the angular resolution of a diffraction limited system. At that point interference effects must be considered and the ray tracing approach no longer suffices. In this case the volume of the last pass approaches $V_o$, the mode volume appropriate to the particular mirror configuration. At the same time the circulating energy reaches a constant value so that the energy increments simply equal the energy emitted on the previous pass, i.e.,

$$\lim_{N \to \infty} \Delta E_{Nn} \to \Delta E_o \, \delta_{Nn} \tag{27}$$

where $\delta$ is the usual delta function. However, the number of passes, N, required for $\omega_N \approx \omega_o$ approaches a thousand for the geometries of interest in these experiments. As a consequence, the 40 - 60 passes observed in the transient system can be accurately treated by the ray-tracing model.

Finally, the average volume for the $N^{th}$ pass given by (26) must be averaged again, weighted by the time - (hence, pass -) dependent intensity observed in the emitted beam. Actual computation of the average volume characterizing a particular measurement requires knowledge of the $\Delta E_{Nn}$ increments and the $V_{Nn}$ volumes. In practice these can be obtained form a tedious but straightforward unfolding process applied to the time-dependent intensity data and normalized by the observed average divergence, $\bar{\omega}$. A ray tracing

program has been written during the current reporting period to perform this unfolding. Necessary input parameters are I(t), the time dependent laser intensity, $\bar{\omega}$ and T, and from these the average volume is calculated from (26) together with the total energy walked-off the mirror and, separately, that re-absorbed when $\Delta E_n < 0$. Generally, this latter consideration is unimportant with re-absorption representing less than 10% of the total extracted energy at 4278 Å. Consequently, this term has been ignored throughout the subsequent analysis. Figure 7 shows the application of the resulting unfolding processes to data typical of that plotted in Figure 5. Quite a variation of functional forms have been measured for I(t), but all lead to average volumes between 17 and 22 $cm^3$. That this unfolding process is meaningful is based on pragmatism. As will be shown below, it reduces the multivariate dependence of all the data obtained to date to form dependent upon a single parameter, the pressure.

For the data at the lower end of Figure 5, to exceed threshold, highly reflective mirrors must be used which greatly raises the ratio of circulating power to emitted power on any particular pass. As a result, walk-off losses are very large and in some cases (P.08) more energy walks-off the mirrors than is emitted. Figure 8 illustrates the effect of considering the total energy extracted from the plasma (i.e., emission + walk-off). The data of the first two cases shown in Figure 7 are presented. Since average volumes are the same in both cases, the effect of walk-off is isolated. As can be seen, the pronounced differences in emitted energy are not found in a comparison of extracted energies.

The same agreement is found in all data taken to date with plane mirror sets, except those oscillating very near threshold (3-4 atm.). This strongly indicates that all of the available energy is being extracted from the plasma by the fields and that the only effect of the varying mirror coefficients is

Figure 7

Summary of various time-dependent, I(t) functions representing the development of the laser output intensity. To the right of each example are shown the characteristic experimental parameters in the order: nitrogen partial pressure in Torr, cavity type (P, plane; H, hemispheric), mirror loss per round trip, and on the subsequent line the corresponding average laser volume calculated by the unfolding program.

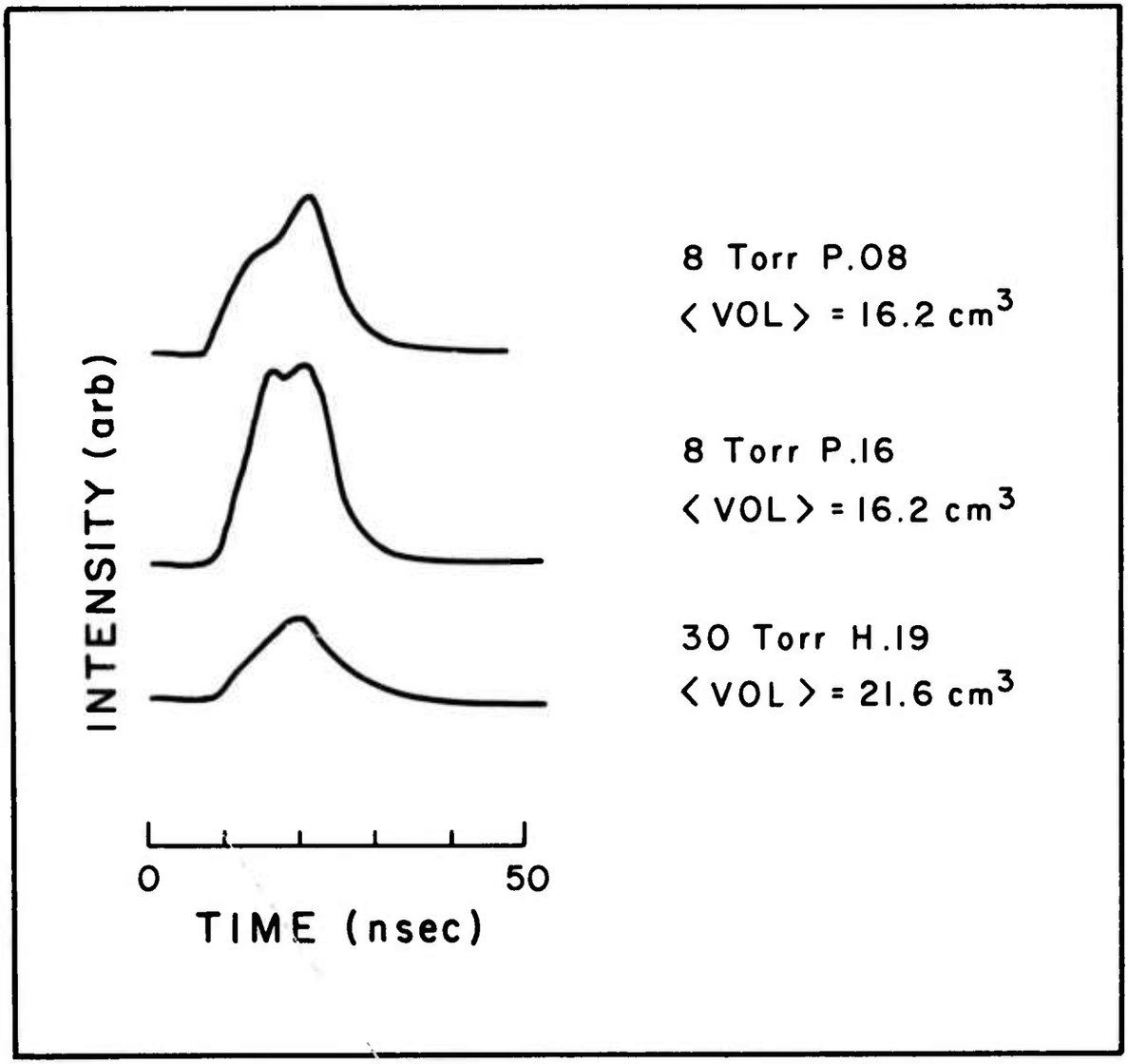
INTENSITY (arb)
8 Torr P.08
⟨ VOL ⟩ = 16.2 cm3
8 Torr P.16
⟨ VOL ⟩ = 16.2 cm3
30 Torr H.19
⟨ VOL ⟩ = 21.6 cm3
0
50
TIME (nsec)

Figure 8

Plots of laser pulse energy as a function of total gas pressure for the data of the first two cases shown in Figure 7. Energy extracted from the plasma is assumed to be emitted energy plus energy walking-off the mirrors. Cavity nomenclature is P.(T) where T is the mirror transparency per round trip.

o Emitted energy, P.08 cavity

Δ Emitted energy, P.16 cavity

× Extracted energy, P.08 cavity

\+ Extracted energy, P.16 cavity

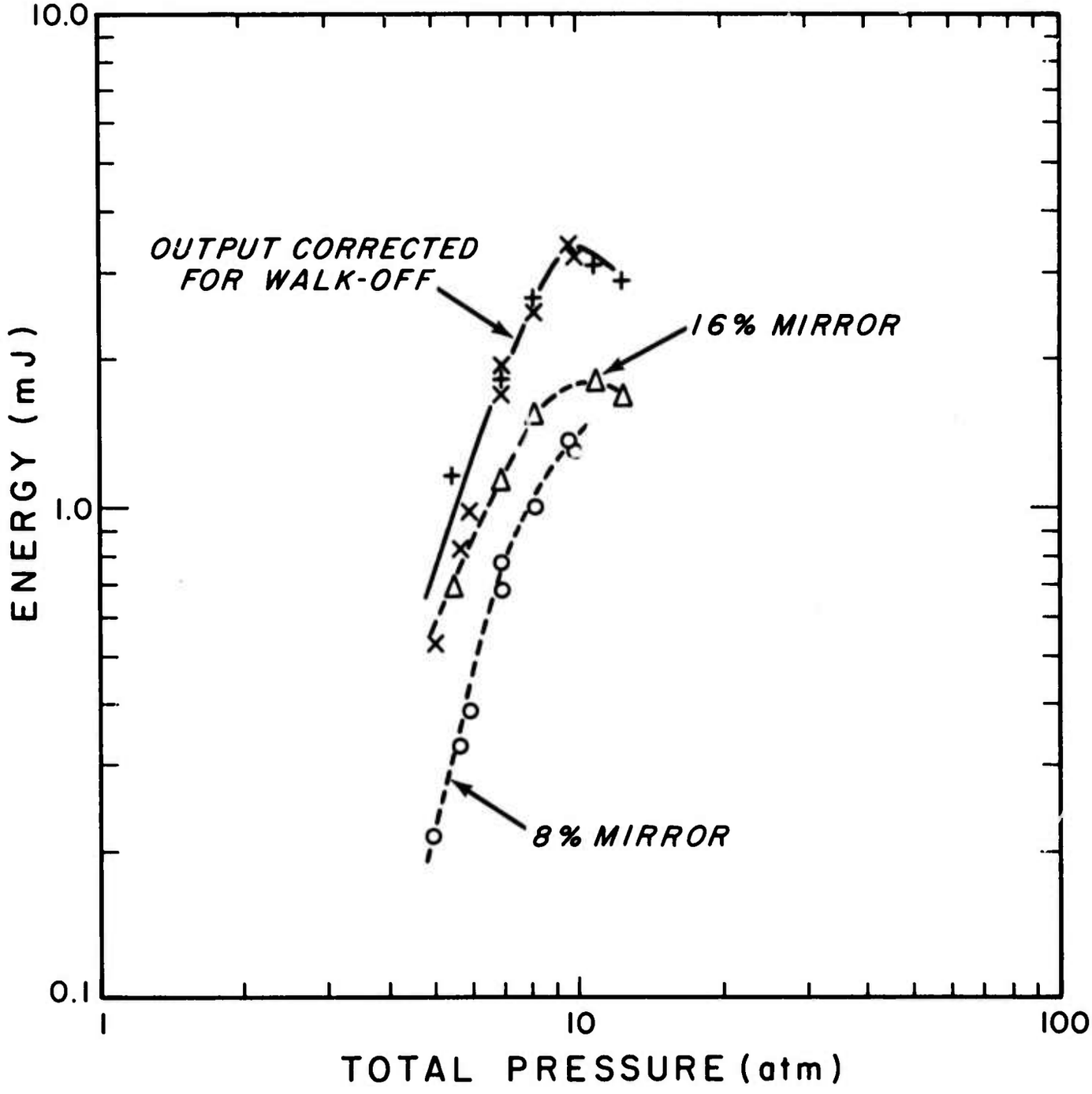
10.0
1.0
0.1
ENERGY (mJ)
OUTPUT CORRECTED FOR WALK-OFF
16% MIRROR
8% MIRROR
1
10
100
TOTAL PRESSURE (atm)

to determine the rate at which that energy is extracted and whether it is routed into the transmitted beam or walks off the mirrors. This is a very important conclusion because it implies competing losses are negligible and that the energy is stored without appreciable degradation in the excited state population until stimulated to emit.

To confirm further the concept that the total energy extracted is independent of mirror parameters, an effort was made to obtain a cavity geometry with low walk-off. Though at this time the unfolding program is only valid for plane parallel cavities, it can be reasonably assumed that for hemispheric cavities with large angular aperture compared to the output beam divergence, ray stability exists for an appreciable region around the cavity axis. For such cavities walk-off could be expected to be negligible in comparison with plane-parallel cavities. For the same plasma conditions, then it could be expected that the energy emitted from a hemispheric cavity would roughly equal the total extracted in either case. Figure 9 presents the data testing this hypothesis. Mirror nomenclature is as before with H denoting hemispheric cavities. For the plane cavities the total of emitted energy and walk-off is plotted and for the hemispheric only emitted energy. Data is plotted in terms of the average mirror loss (not transmission) per round trip transit. Agreement is believed to lie within experimental error and reproducibility of individual measurements.

C. Laser Output and Efficiency at 4278 Å - Data has been collected over a broad span of experimental parameters. Total pressures have ranged from 1 to 30 atmospheres with partial pressures of nitrogen varying from 2 to 120 Torr. As discussed in the previous section, variation of cavity constants affects the rate of energy extraction from the e-beam plasma, but has little

Figure 9

Total energy extracted from the plasma is plotted as a function of round trip mirror loss for the two total pressures shown. Nomenclature beneath each arrow identifies the particular cavity type as H or P, for hemispheric or plane, and the fractional transmission per round trip transit of the cavity. Average cavity loss is larger because of the average walk-off loss per round trip. For P-cavities ordinates correspond to emitted energy plus walk-off while for H-cavities walk-off is assumed negligible and only emitted energy is plotted.

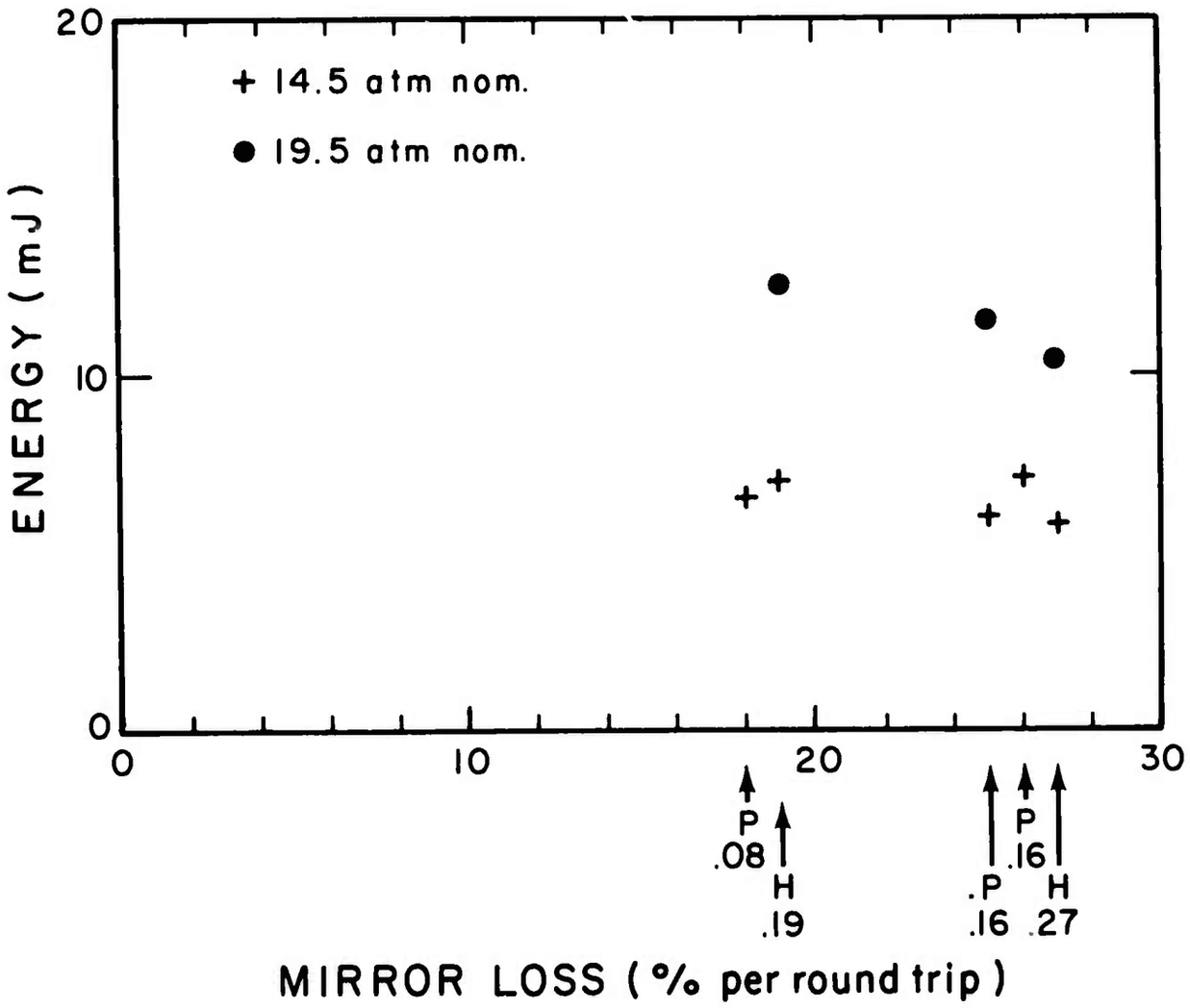
20
10
0
+ 14.5 atm nom.
● 19.5 atm nom.
ENERGY (mJ)
0
10
20
30
P
.08
H
.19
P
.16
.P
.16
H
.27
MIRROR LOSS (% per round trip)

effect on its total. To within rather unrestrictive limits the corrections of the previous section can be employed to reduce the parameterization of the laser performance to depend upon a single variable, total pressure. The limits bounding this parameterization are primarily a consequence of two effects.

1) If the ratio of nitrogen to helium exceeds the limits inferred in Table 3, laser output will be drastically reduced or prevented altogether.

2) If the combination of mirror loss and gas composition is such as to delay the onset of lasing until beam current is beginning to decrease at the end of the e-beam pulse, outputs will again be reduced or terminated. Evidently, in this case. the excited state chemistry is altered by the termination of the beam and competing processes such as recombination with the cooling electrons become important.

Except for data obtained under those conditions, most of the data can be reconciled with a very simple parameterization of the total energy extracted from some standard plasma volume.

The largest laser outputs found in the raw data were from the H.27 cavity and the average volume appropriate to that data was 16.2 $cm^3$. This was chosen as the "standard volume." Since walk-off is assumed zero for the hemispheric cavities, the largest laser outputs (from the 20 - 30 atm. data) simply correspond to unscaled measurements of the total energy emitted into the laser output beam. For the purposes of parameterization, other measurements were scaled to obtain the total energy extracted from a 16.2 $cm^3$ volume of the plasma, so that

$$E_x = (1 + \bar{W}) \times (16.2/\bar{V}) \times E_e \quad , \qquad (28)$$

where $E_e$ is the energy emitted by the cavity into the laser beam, $E_x$ is the total energy extracted from the plasma by the fields, $\overline{V}$ is the average volume from which it was extracted, and $\overline{W}$, the average ratio of energy walking-off the mirrors to that emitted into the beam. As mentioned above, for H-cavities, $\overline{W}$ was assumed to be zero.

The resulting summary of measurements to date is presented in Figure 10. The total energy extracted from the 16.2 $cm^3$ of the charge transfer plasma is plotted as a function of total gas pressure. Data all corresponds to excitation at the level of 78.2 mJ/atm by the discharge pulse shown in Figure 4. The partial pressures of nitrogen varies from 8 to 120 Torr and are indicated by the type of symbol plotted. As can be seen, data groups around a line of slope 2.2. Since the energy input deposited by the beam varies linearly with pressure, the consequent efficiency of energy extraction can be modelled to vary with the 1.2 power of the pressure. An extrapolation of the fit to the data appears to intersect the theoretical limit around 100 atm. so that the efficiency can be conveniently expressed as

$$E = 6.5\% \ (P/100)^{1.2} \quad . \tag{29}$$

The best output to date can be seen to be 36 mJ at 28.7 atm which corresponds to an efficiency of 1.6%.

D. Other Transitions, 3914 Å and 4709 Å - As mentioned in Section II, the Franck-Condon factors for the (0,0) and (0,2) transitions are sufficiently favorable that the threshold should be attained with the proper mirror sets. This was observed to be the case and each transition could be isolated. Figure 11 shows typical outputs in comparison with the (0,1) transition at

Figure 10

Summary plot of total laser pulse energy emitted from a 16 $cm^3$ volume as a function of relative deposition of energy from the electron beam. Units have been chosen so that the deposition is numerically equal to the total gas pressure in atmospheres. Variation of the deposition was obtained by changing the total gas pressure; hence the stopping power. The peak e-beam current was 13 KA in each case. Lines of constant efficiency appear as diagonals with corresponding values marked. Different partial pressures of $N_2$ are indicated by the shape of the data point as follows:

O - 8 Torr

X - 30 Torr

△ - 60 Torr

□ - 120 Torr

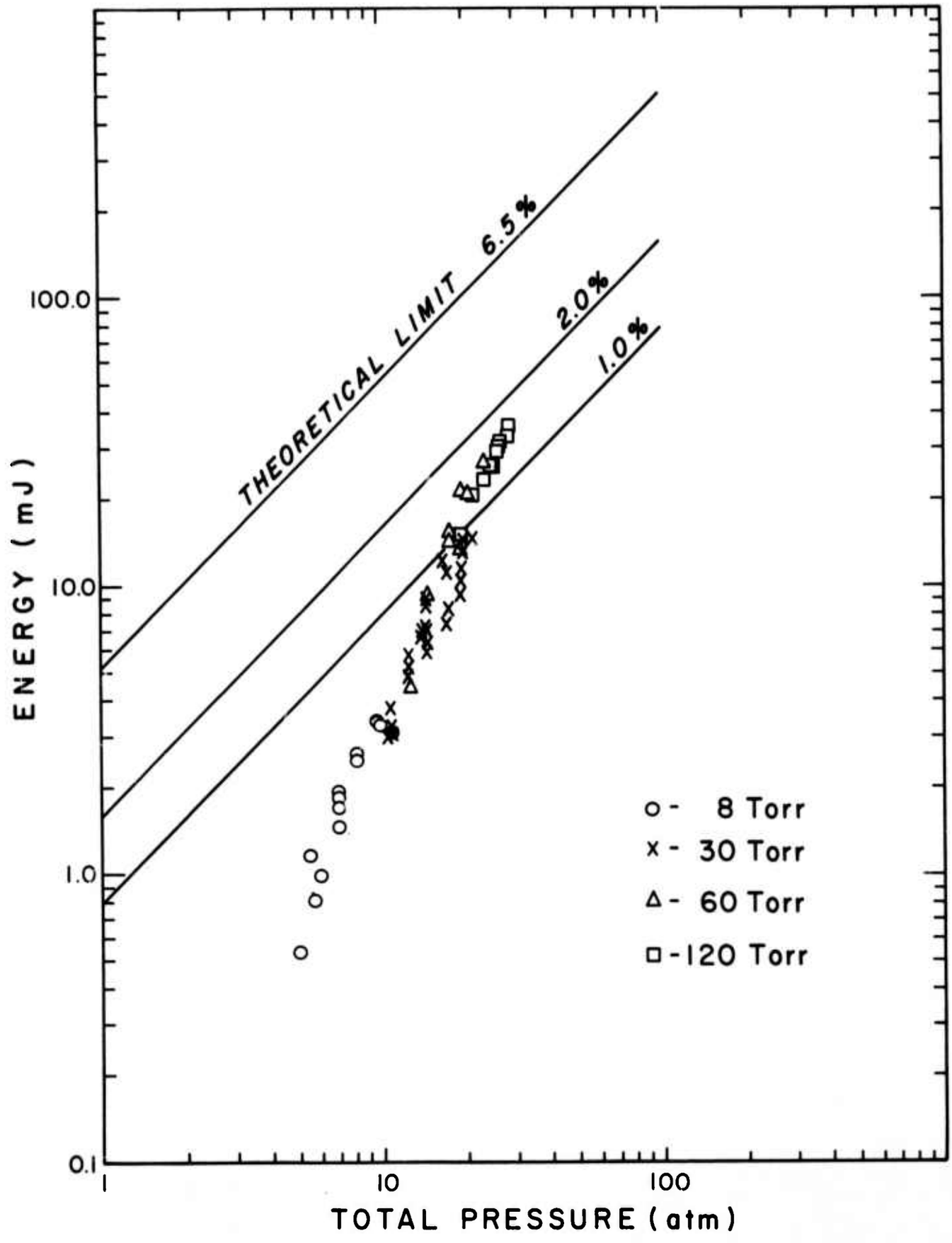
THEORETICAL LIMIT 6.5%
2.0%
1.0%
100.0
10.0
1.0
0.1
ENERGY (mJ)
1
10
100
TOTAL PRESSURE (atm)
o - 8 Torr
x - 30 Torr
Δ - 60 Torr
□ - 120 Torr

Figure 11

Time-resolved power measurements of the nitrogen ion laser outputs for three different mirror sets individually optimizing the (0,0), (0,1), and (0,2) transitions at 3914, 4278, and 4709 A, respectively. Corresponding total pressure are, from top to bottom, 10.8, 14.9, and 16.3 atm. The time scale is as indicated and has been shifted so that the zero corresponds to the beginning of the e-beam current output.

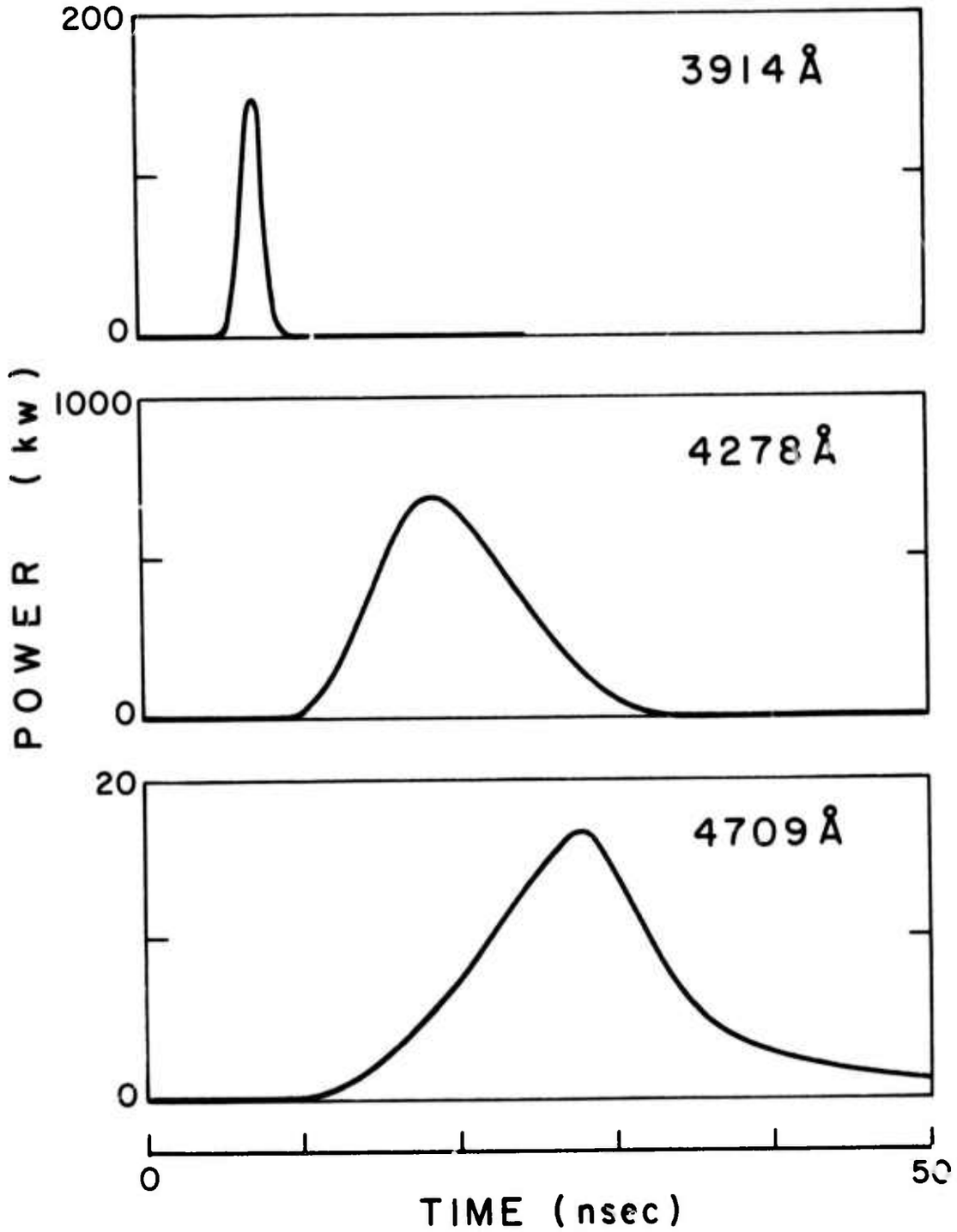
200
3914 Å
0
1000
4278 Å
0
20
4709 Å
0
POWER (kw)
0
50
TIME (nsec)

4278 Å. As would be expected, a priori from the 25:4.4:1 ratio for the Franck-Condon factors from the upper v'=0 state to the lower v"=0,1, and 2 levels, respectively, the onset of threshold was proportionally delayed.

As can be seen, the 3914 Å component self-terminates in about 2 nanoseconds and gives a measure of the time required for the lower laser state to "fill". Since the lower state of the 4278 Å differs only in vibrational quantum number, it has the same degeneracy and should "fill" to terminate the 4278 Å transition in a comparable time. That it does not, as seen in the figure, is strong evidence for the existence of an unblocking process tending to quench the vibrational excitation of the lower, v"=1, state of 4278 Å transition. Further study is needed to characterize and optimize this process to extend the duration of the laser output.

The problem of determining the absolute energy deposition from the electron beam in the radiating volume are particularly acute in the case of the 3914 Å emission. Since the laser output in this case occurs so early in the course of the e-beam pulse, it is misleading to correlate the laser pulse energy with the entire e-beam input energy. Clearly it is only the e-beam energy which is deposited before the termination of the laser pulse that can contribute to the laser excitation. In the case of the 3914 Å output, the procedure was adopted for the purpose of calibrating efficiency of only considering that fraction of the e-beam energy input prior to the termination of the laser output pulse. This is in contrast to the procedure used for the 4278 Å output. As mentioned in Section III A, for determination of those efficiencies the entire e-beam pulse energy was considered input.

Application of the unfolding program to the 3914 Å data gave an average volume of 16.8 $cm^3$ so that the calibration constant for the input energy became 11.0 mJ/atm into this slightly larger "standard volume" for the 3914 Å

data. Because of the drastic difference in the pulse shape of the 3914 Å output two expressions for the energy extracted should be considered. First is the net energy extracted from the plasma, which is the measured output emitted into the beam corrected for walk-off losses according to equation (28). For this case these losses are comparable to those observed for the 4278 Å data at comparably low pressures. Second, however, is the gross energy extracted. This is the net energy plus the energy extracted and subsequently re-absorbed at the end of the laser pulse. This re-absorption loss is also calculated by the unfolding program and in the case of the data of Figure 11, is quite significant. This is again in contrast to the 4278 Å data for which re-absorption was of the order of 7% of the output and, hence, was neglected.

Figure 12 shows a comparison of both net and gross energy extracted from the plasma at 3914 Å as a function of pressure. Lines of constant efficiency are shown and the best efficiency for the gross energy extracted can be seen to have reached 1.5% at 7 atm. of helium and 4.2 Torr $N_2$. Since it is possible that a more transparent mirror set might allow more of the circulating energy to be switched out into the beam and less to be re-absorbed, it is not unreasonable to conclude that the gross extraction shown in Figure 12 is a scalable measure of performance for the laser at 3914 Å.

Unfortunately, a lack of variability in available mirror coefficients prevented an extensive examination of either the 3914 Å or 4709 Å output characteristics during the current reporting period. Procurement of a more extensive mirror set is planned and it is intended to characterize the (0,0) and (0,2) transitions more adequately.

Figure 12

Summary plot of total laser pulse energy extracted from a 16.8 $cm^3$ volume at 3914 Å as a function of total pressure. Lines of constant efficiency appear as diagonals as marked.

0 Net energy extracted

\+ Gross energy extracted and corrected for the re-absorption of the energy circulating in the cavity at the end of the pulse

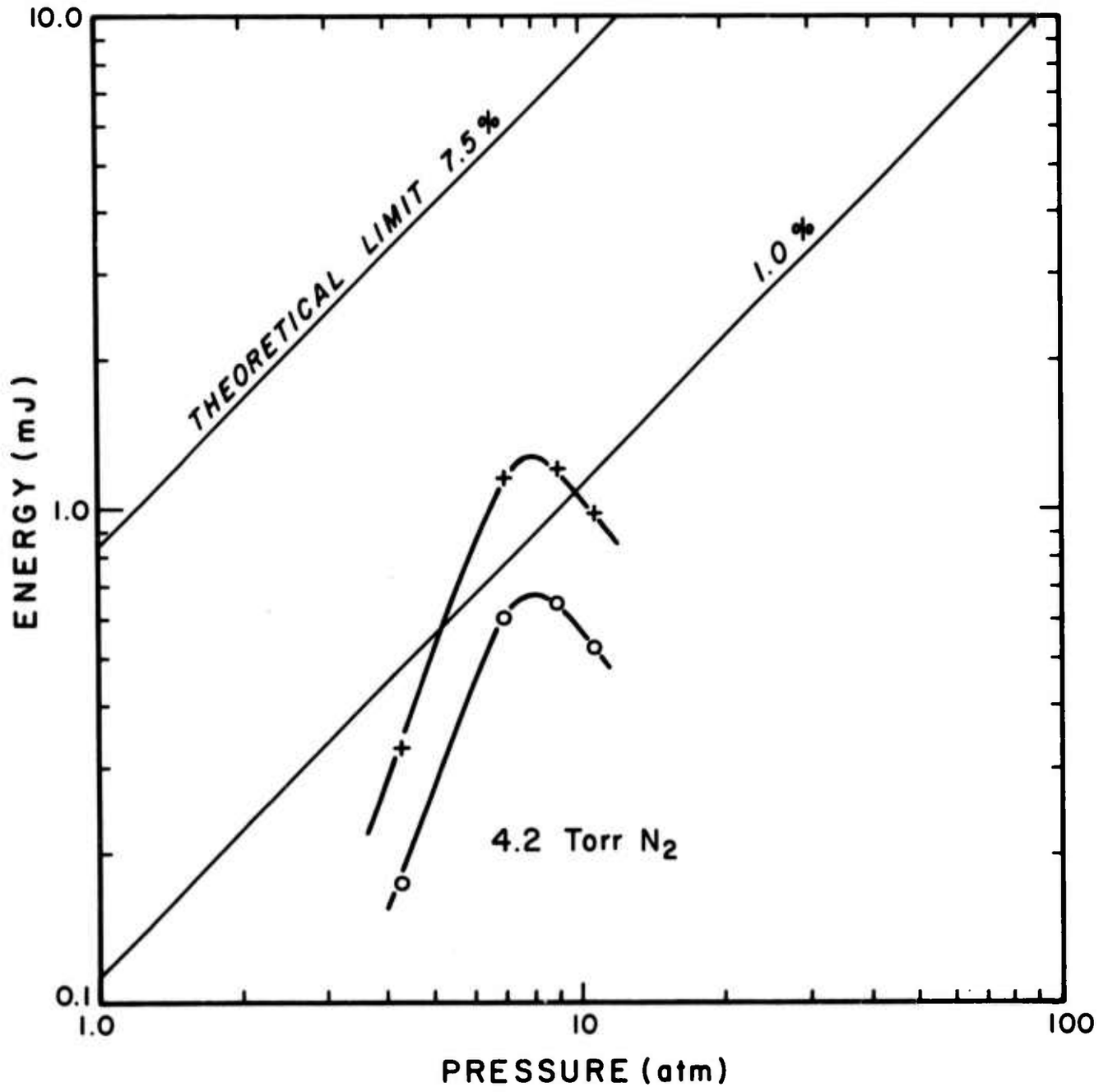
10.0
1.0
0.1
ENERGY (mJ)
THEORETICAL LIMIT 7.5%
1.0%
4.2 Torr $N_2$
1.0
10
100
PRESSURE (atm)

## IV. IMPLICATIONS

The high efficiency already observed in the emission of the single line at 4278 Å from the first nitrogen ion laser confirms the importance of the charge transfer pumping mechanisms proposed by the Principal Investigator and co-workers.[1] Moreover, it points toward the development, in the visible wavelength region, of new types of high energy lasers depending upon charge transfer from electron beam excitation of analogous high pressure gas mixtures. It should be emphasized that it is reasonable to expect that this will ulitmately lead to the construction of lasers operating with efficiencies between 5 and 10% at a variety of wavelengths in the visible region.

More immediate implications concern the further scaling of the current nitrogen charge-transfer laser. It now appears that the theoretical efficiency of 6.5% for the 4278 Å transition will be attained at operating pressures around 100 atm. Even at the relatively low operating current of 13 KA currently used, this will yield a deposition of 483 J/liter and an output of 31 J/liter. The larger ELAC-2 laser device under construction will test these projections.

Since the APEX-1 e-beam gun is nominally a 10Ω device, it should be capable of discharging 100 KA into a beam 4 cm x 20 cm. In that case, an afterglow chamber having 40 cm optics would support the extraction of energy from a 3.2 liter volume. Then the principal problem to excitation would be simply a mechanical one of containing the pressure across a large output aperture. The primary implication of the work reported here is that if these mechanical problems could be satisfactorily resolved, a 100 Joules output at 4278 Å could be realized from current electron beam technology.

It is further reasonable to expect that this energy can be switched into other radiative channels from the same upper state through the use of mirror sets of appropriate reflectivity at the desired wavelength and suitably transparent at the others. Since the three potentially useful wavelengths lie at 427, 471 and 523 nm, they are sufficiently separated that fabrication of such mirror sets should present no technological problem.

Finally, it appears that, if development along those lines appeared warranted, a visible laser of exceptionally high average power could be pumped by charge transfer. Assuming, again, that the test laser system proves scalable, it can be expected that some type of sustainer excitation could be arranged to pump of the order of 5 liters at the 1.3 $KA/cm^2$ current density with a repetition rate of 100 pps. Then, at 30 atmospheres pressure a laser with 1 KW average power at 4278 Å could be realized with currently demonstrated levels of efficiency.

While such projections are, of course, speculative, these are the implications of the recent successes with the scaling of the first nitrogen ion laser discussed in this report.

## V. REFERENCES


1. C. B. Collins, A. J. Cunningham, S. M. Curry, B. W. Johnson and M. Stockton, Appl. Phys. Lett. 24, 477 (1974).

2. C. B. Collins, A. J. Cunningham and M. Stockton, Appl. Phys. Lett. 25, 344 (1974).

3. C. B. Collins and A. J. Cunningham, The Nitrogen Ion Laser, Special Technical Report, UTDP-ML-01 (1974).

4. C. B. Collins and A. J. Cunningham, The Nitrogen Ion Laser, Fifth Semi-Annual Technical Report, UTDP-ML-02 (1974).

5. J. B. Gerardo and A. W. Johnson, I.E.E.E., J. Quant. Elect. QE-9,748 (1973).

6. M. L. Bhaumik and E. R. Ault, U.V. Gas Laser Studies Special Technical Report (Northrop Corp. NRTC. 73-16R, (1973).

7. R. W. Dreyfus and R. T. Hodgson, Appl Phys. Lett. 20, 195 (1972).

8. R. T. Hodgson and R. W. Dreyfus, Phys. Rev. Lett. 28, 536 (1973).

9. D. A. Hammer and N. Rostoker, Phys. Fluids 13, 1831 (1970)

10. R. V. Lovelace and R. M. Sudan, Phys. Rev. Lett. 27, 1256 (1971).

11. G. Knop and W. Paul, in: Alpha, Beta and Gamma-Ray Spectroscopy (ed. Kai Siegbahn, North-Holland Co., Amsterdam, 1965), p 1-25.

12. W. P. Jesse and J. Sadauskis, Phys. Rev. 97, 1668 (1955).

13. C. B. Collins and W. W. Robertson, J. Chem. Phys. 40, 701 (1964).

14. R. A. Gerber, G. F. Sauter and H. J. Oskam, Phys. Lett., 19, 656 (1966).

15. D. K. Bohme, N. G. Adams, M. Mosesman, D. B. Dunkin, and E. E. Ferguson, J. Chem. Phys. 52, 5094 (1970).

16. F. C. Fehsenfeld, P. D. Goldan, A. L. Schmettekoph, H. I. Schiff, and E. E. Ferguson, J. Chem. Phys. 44, 4087 (1966).

17. G. Herzberg, Molecular Spectra and Molecular Structure: I. Spectra of Diatomic Molecules (Van Nostrand, Princeton, N. J., 1950), p. 21.

18. D. C. Tyte and R. W. Nichols, Identification Atlas of Molecular Spectra, University of W. Ontario, Dept. of Physics, Molecular Excitation Group, London, Ont. 1965 p. 14.

19. G. Herzberg, op. cit., p. 125.

20. G. Herzberg, op. cit., p. 554.

21. R. W. Nicholls, J. Res. NBS, 65A, 451, (1961).

22. M. L. Bhaumik, E. R. Ault, and N. T. Olson, U.V. Gas Laser Investigations Semiannual Technical Report (Northrop Corp. NRTC. 74-70R, (Nov. 1974).